

Galactic Metallicity Gradients Derived from a Sample of OB Stars

Simone Daflon

*Observatório Nacional, Rua General José Cristino 77
CEP 20921-400, Rio de Janeiro Brazil*

`daflon@on.br`

Katia Cunha

*Observatório Nacional, Rua General José Cristino 77
CEP 20921-400, Rio de Janeiro Brazil
and*

*Department of Physics, University of Texas at El Paso
El Paso, TX 79968-0515*

`katia@baade.physics.utep.edu`

ABSTRACT

The distribution of stellar abundances along the Galactic disk is an important constraint for models of chemical evolution and Galaxy formation. In this study we derive radial gradients of C, N, O, Mg, Al, Si, as well as S, from abundance determinations in young OB stars. Our database is composed of a sample of 69 members of 25 open clusters, OB associations and H II regions with Galactocentric distances between 4.7 and 13.2 kpc. An important feature of this abundance database is the fact that the abundances were derived self-consistently in non-LTE using a homogeneous set of stellar parameters. Such an uniform analysis is expected to reduce the magnitude of random errors, as well as the influence of systematics in the gradients defined by the abundance and Galactocentric distance. The metallicity gradients obtained in this study are, in general, flatter than the results from previous recent abundance studies of early-type stars. The slopes are found to be between -0.031 (for oxygen) and $-0.052 \text{ dex kpc}^{-1}$ (for magnesium). The gradients obtained for the studied elements are quite similar and if averaged, they can be represented by a single slope of $-0.042 \pm 0.007 \text{ dex kpc}^{-1}$. This value is generally consistent with an overall flattening of the radial gradients with time.

Subject headings: stars: abundances — stars: early-type — Galaxy: abundances — Galaxy: evolution

1. Introduction

Chemical evolution models of the Galaxy must reproduce certain observational constraints, such as the age-metallicity relation, the abundance patterns of different stellar populations and the chemical composition of the Sun. Reliable observational data for a variety of objects (where observational data in this case means results from abundance analyses) are thus crucial in constraining the assumptions that enter in the construction of such models. One very important observational model constraint is the radial metallicity gradient, or, the distribution of abundances in the Galactic disk as a function of Galactocentric distance, R_g . In general terms, abundance gradients are a feature commonly observed in all galaxies with their metallicities decreasing outwards from the galactic centers. Metallicity gradients appear to be shallower in elliptical galaxies and progressively increase from lenticulars to barred spirals, being steeper in normal spirals. (See e.g. the review by Henry & Worthey 1999). For these extragalactic systems the metallicity is traced via analyses of individual H II regions (Vila-Costas & Edmunds 1992; Kennicutt, Bresolin & Garnett 2003) and by the most luminous stars in galaxies of the local group (e.g. Monteverde et al. 1997), or by photometric properties. In our own Galaxy, metallicity gradients can be determined via abundance analyses of ionized gas in H II regions and planetary nebulae, chemical compositions of stellar photospheres of young OB stars and the more evolved Cepheids, or from studies of metallicities of open clusters. Although significant efforts have been put into trying to pin down metallicity gradients for the Galactic disk, the abundance slopes for the different elements in these different populations remain somewhat uncertain.

Focusing first on metallicity gradients inferred from analyses of young OB stars, there seems to be no consensus between the different determinations published over the last 10–15 years. The first studies of Fitzsimmons et al. (1990) suggested almost null gradients of oxygen and magnesium, while for N, Al and Si they found a tendency of increasing abundances with Galactocentric radius. Later on, Kaufer et al. (1994) combined their own abundance determinations of N and O with those from the literature and obtained a zero gradient for oxygen and $-0.026 \text{ dex kpc}^{-1}$ for nitrogen. Kilian-Montenbruck, Gehren, & Nissen (1994) derived abundance gradients for several elements (C, N, O, Mg, Al, Si in non-LTE and Ne, S, Fe in LTE) that were in general flatter than $-0.03 \text{ dex kpc}^{-1}$ in the range between $R_g = 5\text{--}15 \text{ kpc}$. (Moreover, their results suggested that the abundance distribution in the local ISM is inhomogeneous.) More recent studies, however, obtained considerably steeper gradients for the Galactic disk. The self-consistent non-LTE study of 16 target stars by Gummersbach et al. (1998) resulted in a gradient of $-0.067 \text{ dex kpc}^{-1}$ for oxygen; for other elements (such as C, N, Mg, Al, and Si), the gradients varied between $-0.035 \text{ dex kpc}^{-1}$ (for carbon) and $-0.107 \text{ dex kpc}^{-1}$ (for silicon). Smartt & Rolleston (1997) compiled data for early-type stars from abundance papers previously published by their group and obtained

an oxygen gradient of $-0.07 \text{ dex kpc}^{-1}$. Other elements like C, N, Mg, Al, and Si, and oxygen included, were analyzed by Rolleston et al. (2000), who found gradients that are steep, but are all similar in magnitude, with a mean value of $-0.068 \text{ dex kpc}^{-1}$. This stellar database was later extended towards the innermost disk by Smartt et al. (2001), providing gradients consistent with those derived by Rolleston et al. (2000) for the disk, except for oxygen.

Several studies of the Milky Way metallicity gradients are based on chemical analyses of ionized gas in H II regions and planetary nebulae. Oxygen abundances for a sample of 21 H II regions between 5.9 and 13.7 kpc by Shaver et al. (1983) indicate a radial gradient of $-0.07 \text{ dex kpc}^{-1}$. Other nebular studies concentrate on specific parts of the Galactic disk. In the outer disk, for example, Vílchez & Esteban (1996) suggest that the N, O, and S gradients are much flatter – when compared to Shaver et al. (1983) – in the direction of Galactic anti-center. Afflerbach, Churchwell, & Werner (1997) studied the region inner to $R_g \sim 11.4 \text{ kpc}$ and obtained gradients for N, O, and S, of about $-0.07 \text{ dex kpc}^{-1}$. However, the most recent nebular studies tend to find flatter gradients for oxygen. Deharveng, Peña, & Caplan (2000) obtained a gradient of $-0.039 \text{ dex kpc}^{-1}$ for oxygen in H II regions between $R_g = 5-15 \text{ kpc}$. Pilyugin, Ferrini, & Shkvarun (2003) did a compilation of spectra from H II regions located between 6.6 and 14.8 kpc and obtained a gradient of $-0.048 \text{ dex kpc}^{-1}$. The planetary nebulae (PNe) ejected from low- to intermediate-mass stars can also trace the abundance gradients. The study of Maciel & Quireza (1999), based on abundance data compiled from the literature, found gradients of $-0.058 \text{ dex kpc}^{-1}$ for oxygen and $-0.077 \text{ dex kpc}^{-1}$ for sulfur. Martins & Viegas (2000) recomputed temperatures and abundances from line ratios published in the literature and obtained -0.054 and $-0.064 \text{ dex kpc}^{-1}$ for oxygen and sulfur, respectively. More recently, however, the analysis of PNe by Henry, Kwitter & Balick (2004) derived flatter gradients of -0.037 ± 0.008 and $-0.048 \pm 0.0098 \text{ dex kpc}^{-1}$ for O and S, respectively.

In fact, the actual picture seems to be more complex as studies of metallicities in open clusters with different ages (Friel et al. 2002; Chen, Hou, & Wang 2003) and abundances of planetary nebulae (Maciel, Costa & Uchida 2003) suggest that the metallicity gradients may evolve, showing a tendency of becoming flatter with time. Besides, there may be a discontinuity in the radial Galactic gradient with two distinct metallicity zones in the disk (results from open clusters from Twarog, Ashman, & Anthony-Twarog 1997 and Cepheids by Caputo et al. 2001; Andrievsky et al. 2004). Concerning the population of young OB stars, a determination of radial gradients that is based on a homogeneous and self-consistent non-LTE abundance database would represent a significant advancement. This is the goal of this paper: the last in a series. In this study we assemble our previous results (Paper I - VI; where we progressively built a non-LTE abundance database of OB stars from high-resolution spectra), in order to better define the current metallicity gradients of the Milky

Way disk.

2. The Abundance Database

Our observational data consisted of 35 high resolution echelle spectra obtained with the 2.1m telescope at the McDonald Observatory (University of Texas, Austin) and 34 obtained with the 1.52m telescope at the European Southern Observatory (La Silla, Chile). Our Northern sample was composed basically of stellar members of nearby OB associations, within 2.5 kpc from the Sun, while the sample stars observed from the South were distributed along the Galactic disk ranging from 4.7 to 13.2 kpc in Galactocentric distance.

Our database contains non-LTE abundances of C, N, O, Mg, Al, Si, and S for 69 late-O to early-B type star members of 25 OB associations, open clusters or H II regions (Papers I–VI), plus 18 stellar members of the Orion association from Cunha & Lambert (1994). All these abundances were derived with the same methodology and are strictly on the same scale. We observed several stars per cluster or association in order to sample, although to a very modest degree, a cluster’s metallicity distribution. Our observing campaigns included 108 additional stars that had to be discarded due to their large projected rotational velocities (the distributions of $v \sin i$ values for our whole sample of stars members of associations will be the subject of a future study), or because they were binary. The association of Cep OB2 was the most extensively probed, with 17 targets analyzed for abundances; for 14 other clusters we had five or less sample stars while for ten others we had to rely on the abundance derived for one target star in order to represent the cluster abundance. Average abundances for each cluster are listed in Table 1, together with the number [n] of stars analyzed in each cluster.

3. The Adopted Distances

Galactocentric distances are a crucial ingredient in establishing radial metallicity gradients. Table 2 lists our target clusters, their Galactic coordinates (columns 2 and 3), and their distances from the Sun (column 4), which were collected from different studies in the literature. Most of these distances were derived from color-magnitude diagrams or from spectral type *vs.* intrinsic color calibrations. In addition, distances from HIPPARCOS parallaxes are available for our nearest target stars that belong to the Ori OB1, Lac OB1 and Cep OB2 associations (de Zeeuw et al. 1999). The typical errors of the distances from the Sun are inferred to be of the order of 10–20% in the individual studies, but can reach 40% in a few

cases. An inspection of different literature values for a given cluster shows that the different distance estimates for some clusters are quite discrepant. The largest dispersions (sigmas between 20-50 percent) are found for NGC 6204, NGC 6604, Vul OB1, NGC 4755, Cep OB2, Sh2 247, NGC 1893 and Sh2 285. The latter, being the furthest H II region in our sample, deserves special mention, as it plays an important role in the definition of the abundance gradient. Lahulla (1987) considered 5 stars in this HII region, and obtained a spectroscopic distance of 6.4 kpc. Moffat, Fitzgerald, & Jackson (1979) derived $d=6.9$ kpc based on UBV photometry and spectral types of two stars; the same distance was obtained by Turbide & Moffat (1993) from the fitting of theoretical isochrones for eight stars. However, Rolleston, Dufton, & Fitzsimmons (1994) derived a smaller distance of $d=4.3$ kpc, based on theoretical evolutionary tracks for two stars in Sh2 285. Here, we adopt the average distance of 5.9 ± 1.4 kpc for Sh2 285. For each target cluster we calculated average distances and dispersions from all the distance estimates. These average distances are listed in column 5 of Table 2.

With the cluster distances from the Sun, d , Galactocentric distances projected onto the Galactic plane can be calculated from

$$R_g^2 = R_\odot^2 + (d \cos b)^2 - 2R_\odot d \cos l \cos b,$$

where R_\odot is the Galactocentric distance of the Sun and l, b are the Galactic longitude and latitude of the object, respectively. Here, the distance of the Sun from the Galactic center is taken to be 7.9 kpc (MacNamara et al. 2000; this value agrees well with the weighted average previously calculated by Reid 1993 computed from published values derived from various approaches, $R_\odot = 8.0 \pm 0.5$ kpc).

The derived cluster Galactocentric distances and uncertainties are listed in column 6 of Table 2; these will be adopted in the gradient calculations. The errors in R_g were computed by noting that these distances depend upon the solar Galactocentric distance, the distance from the Sun to the cluster (d), and the cluster Galactic latitude and longitude. The total uncertainty then consists of the quadratic sum of the products of each of these quantities by the corresponding uncertainties. In Figure 1 we show the space distribution of our sample and the positions of the sample clusters (open circles) projected onto a section of the Galactic plane. The range in Galactocentric distance spanned by the different determinations in the literature for each cluster are represented by the bars in each location (the bar sizes are set by the smallest and largest distances in each case). Our database samples the inner arm of Sagittarius-Carina (objects within $295^\circ < l < 360^\circ$ and $360^\circ < l < 18^\circ$), the extension of the Perseus arm ($174^\circ < l < 214^\circ$, with distances larger than 1.5 kpc), as well as the local Orion spur ($40^\circ < l < 206^\circ$), where the Sun lies (Han et al. 2002, after Georgelin & Georgelin 1976).

4. The Radial Gradients

One of the simplest ways to represent the distribution of radial metallicities across the Galactic disk is to assume that abundance trends can be represented by straight lines spanning the whole interval in Galactocentric distance covered by the sample. Radial metallicity gradients can then be obtained from linear fits of the form $a + bx$ to the abundances as a function of Galactocentric distances; the abundance gradient, therefore, being represented by the single coefficient b . From our database of C, N, O, Mg, Al, Si and S abundances for clusters and associations (Table 1) and their Galactocentric distances (Table 2), best-fit straight lines ($a \pm \sigma a$ and $b \pm \sigma b$) and correlation coefficients (R) were calculated. These are listed in Table 3 together with the number, n , of clusters or associations considered for each element. Here, the gradients were calculated assuming that the cluster abundances are represented by *averages* of the abundances obtained for their sample stars.

The derived slopes (b values) are negative for all elements and indicate that, as expected, the abundances decline with Galactocentric distance but the decline is not very steep. In addition, it seems that the gradients do not vary significantly and can be considered to be approximately the same for all studied elements: they can be represented by an average slope of $-0.042 \pm 0.007 \text{ dex kpc}^{-1}$. In the different panels of Figure 2, we display the abundance gradients obtained for each element. Horizontal errorbars represent the adopted uncertainties in R_g and the vertical ones the abundance dispersions for each cluster. For comparison, we also show the most recent solar abundance results at the Galactocentric distance of 7.9 kpc. It is clear that these solar results fall within the OB-star abundance distributions obtained for the studied elements at the solar radius; except for aluminum whose distribution is below solar by roughly 0.3 dex.

Meaningful radial gradients can be also computed considering the individual abundances derived for each sample star. One of the advantages being that one can then isolate subsamples of stars in order to investigate the existence of possible systematic effects in the derived gradients. For instance, a subsample of stars selected to span a very narrow range in effective temperature can minimize the effects of systematics in the obtained abundances. Another possibility is to segregate the sample in subsamples of sharp-lined and broad-lined stars in order to check if there are systematic differences in the obtained abundances and corresponding gradients. In the following, these two cases are discussed.

Subsample of Stars within a Restricted Range in T_{eff} : Ideally, to minimize the influence of systematic errors, Galactic radial metallicity gradients should be obtained from samples of stars within a very narrow range in stellar parameters. However, it is very difficult to assemble a large sample of sharp-lined early-type stars if a very restricted range

in effective temperature is imposed. Although this was one of our original goals, our final sample covers quite a large range in effective temperature from roughly 19 000 to 34 000 K; probably different systematic errors are affecting the abundances in the stars at the “cool” and “hot” end of our sample.

A subsample defined to have a narrower range in effective temperature was constructed by adopting as optimum temperature (T_{\max} ; center of the subsample distribution) the one for which the line strengths of a given ion reach a maximum. In these regimes, the abundances are rather insensitive to changes in T_{eff} and in this sense, those stars with temperatures close to T_{\max} are expected to present the most reliable abundance results. As a consequence, gradients derived from subsamples of stars within a narrow range in T_{eff} around T_{\max} are expected to be more robust, even if the “real” T_{eff} for the star is relatively lower or higher than the value adopted in the abundance analysis. Given T_{\max} for each element (except Mg; Mg II triplet at 4481Å reach a maximum at temperatures around 10 000 K) we assembled subsamples with stars of effective temperatures within a 2σ interval around T_{\max} ; where $\sigma \sim 4\%$ is estimated to be the uncertainties in the T_{eff} -scale adopted in our abundance analyses (see discussion in Paper I). The stellar subsamples considered for each studied element are shown as filled circles in the panels of Figure 3, while the remaining stars in our sample are represented by open circles. The corresponding gradients are shown for comparison. For oxygen, in particular, the similarity of the slopes (represented by solid and dotted straight lines) indicates that the two gradients are practically indistinguishable, with no indications that significant systematic effects are introduced when the full sample, which has a large range in T_{eff} , is considered: the results for oxygen seem therefore very robust. For all other elements, however, there is a tendency of finding slightly flatter gradients when subsamples with T_{eff} around T_{\max} are adopted. These flatter gradients for C, N, O, and Si are all consistent with our original values within the expected errors. The changes in the gradients of Al and S derived for the restricted sample in T_{eff} exceed the expected uncertainties.

Subsample of Stars with Low $v \sin i$: Our abundance database includes mostly sharp-lined stars (with relatively low $v \sin i$) but, because we adopted spectral synthesis technique throughout our abundance analyses, it also includes 26 OB stars with $v \sin i > 60 \text{ km s}^{-1}$; all these fast rotators are located within 9 kpc from the Galactic center and populate the inner part of the Galactic disk. The abundances of broad-lined, rapidly rotating stars are expected to be somewhat more uncertain than the sharp lined stars, due to line blending. In addition, effects of changes in the abundances due to rotation are more likely to be influencing the high $v \sin i$ stars, so it is useful to investigate if the high $v \sin i$ stars in our sample could be introducing an unexpected bias in the derived abundance gradients.

Observational evidence that mixing occurs in our sample was discussed in Paper III: N overabundances were observed in two of the most massive, most evolved, and most rapidly rotating (highest $v \sin i$) members studied in the Cep OB2 association. These abundance changes due to mixing raise the question of whether the inclusion of high $v \sin i$ stars in our sample could be affecting systematically the C, N and perhaps O abundance gradients obtained. This possibility is investigated here by segregating our sample in subsamples of stars with low and high $v \sin i$ and computing the corresponding gradients. In the three panels of Figure 4 the sample stars with high $v \sin i$ are represented by open circles, while low $v \sin i$ stars are filled circles. We show, for C, N and O, two different abundance gradients: one obtained for our complete sample (represented by dotted lines) and another that was computed only for those 43 stars with $v \sin i < 60 \text{ km s}^{-1}$ (represented by solid lines). The conclusion is that the derived slopes are not significantly different; or that the abundance distribution obtained from analyses of high $v \sin i$ stars in our sample are in general agreement with what is obtained for the sharp lined ones. However, as we do not know the actual velocity of rotation for the stars, but only their projected rotational velocity, a fraction of the stars that have sharp lines in our sample are also fast rotators seen pole on, so these two populations are actually mixed in the sharp lined sample.

4.1. Gradients from the Sample Binned in R_g

Our database of OB stars from open clusters, OB associations and H II regions plus Orion, covers 26 disk positions within a range in Galactocentric distance between 4.7 and 13.2 kpc. The targets, however, are not homogeneously distributed along the disk. As can be seen from the distribution of abundance points in Figure 2, our sample is heavily weighted towards the inner disk and more scarcely sampled outwards. Fourteen clusters have $R_g < R_\odot$ and lie inside the circle described by the Solar orbit. Five OB associations (Cep OB2, Cep OB3, Cyg OB7, Ori OB1, and Lac OB1) lie very close to the Sun and are considered also as part of the inner disk. On the other hand, the chemical distribution of the outer disk is represented by abundances of only 9 stars that are members of 7 clusters.

In order to test if a distribution homogeneously sampled would result in significantly different gradients, we divided our sample in 9 bins of 1 kpc each (between $R_g = 4$ and 14 kpc) and calculated average abundances and Galactocentric distances considering those targets available in each bin. In Figure 5 we represent, for each bin, the average abundances and distances as solid circles. New abundance gradients were then calculated for this binned sample and these are shown as solid straight lines in the figure. For comparison, we also show the original gradients (derived previously and based on average abundances per cluster) as

straight dotted lines. A comparison of the best-fitted lines in each panel of Figure 5 indicates that the new gradients are not significantly different from the original ones, but we note, that there is a tendency of finding slightly flatter gradients when the sample is binned. The new C, N, Mg, Al, and S gradients are shallower than the original gradients with typical differences of -0.01dex kpc^{-1} ; the changes in the gradients of O and Si are smaller than $-0.005\text{dex kpc}^{-1}$.

5. Discussion

The derived radial gradients from our database of C, N, O, Mg, Al, Si and S abundances are summarized in Table 3. The main result being that the metallicity gradients in the Milky Way disk are relatively flat, with an average slope of $-0.042\text{dex kpc}^{-1}$. All our efforts in the sense of trying to minimize systematic errors (by binning the sample and isolating subsamples of stars for which it is expected that the derived abundances would be most reliable) led to gradients that were, in all cases, flatter than the results in Table 3. Therefore, there seems to be significant support that, from this sample of OB stars, the radial metallicity gradients are not steep. In particular, these flatter gradients are generally in line with the fact that the Milky Way seems to be a spiral galaxy having a bar of ~ 3.5 kpc in its Galactic center (Weiner & Sellwood 1999; Bissantz & Gerhard 2002). The observed gradients among spirals show a correlation with the presence and length of a central bar: there is a tendency of finding steeper gradients in normal spiral galaxies when compared to barred spirals (Martin & Roy 1994), as the bar would act as to promote the homogenization of the Galactic chemical composition, especially in the region of the inner disk.

Some interesting abundance patterns seem to emerge from the trends of abundance with Galactocentric distances presented in this study. It seems that a few objects in our sample have abundances that deviate from the best-fitted slopes, being significantly lower than average by an amount larger than the expected uncertainties. In the following, we evaluate how much the elemental gradients would change if one simply rejected from our sample those clusters whose abundances are the lowest, and most discrepant in each case.

For nitrogen, magnesium and perhaps sulfur, the association of Mon OB2, at a Galactocentric distance of ~ 9.4 kpc, has lower abundances than expected given its Galactocentric distance. The metallicity of this OB association, however, is represented by the abundance of only one star, HD 46202 (analyzed in Paper VI). Exclusion of this low abundance star would not significantly change the obtained gradients: the new gradients without Mon OB2 are -0.032 , -0.046 , and $-0.033\text{dex kpc}^{-1}$, for N, Mg and S, respectively. For silicon, the abundance of Monoceros OB2 is not discrepant. The lowest Si abundances, however, are

found for the two stars members of the open cluster NGC 2414. When these are discarded, the Si gradient is flattened to $-0.032 \text{dex kpc}^{-1}$.

For oxygen, the situation seems more intriguing as there are four stars in our sample with significantly lower oxygen abundances, all of them lying between 9.4 and 10.9 kpc away from the Galactic center: HD 46202 (from Mon OB2), the two targets in NGC 2414, as well as the exciting star of the H II region Sh2 247. These objects belong to the only three clusters/associations in our sample that fall between $R_g = 9$ and 11 kpc, and they have an average oxygen abundance of 8.11 ± 0.07 , or, 0.55 dex lower than the solar value. Our tests indicate that if HD 46202 and Sh2 247-1 are discarded one at a time, the oxygen gradient remains approximately unchanged. However, if we discard the stars in NGC 2414, the gradient flattens to $-0.024 \text{dex kpc}^{-1}$. This simple exercise shows that these low abundance stars in NGC 2414 are playing an important role in making the oxygen gradient steeper. It should be stressed here, however, that the abundance results for these two stars seem quite solid, they both give consistently low values, and we see no reason why their abundances should be more uncertain. In fact, their effective temperatures ($T_{\text{eff}} = 23\,260$ and $28\,140$ K) are such that their abundances should be considered more robust, since the latter are quite insensitive to errors in the T_{eff} . (We note that these two stars were included in the oxygen subsample defined around T_{max} and discussed in Section 4.)

As discussed previously, the derived gradients are also subject to uncertainties in the adopted distances to the target clusters, and these were taken into account in the determination of the best-fitted slopes. Here, in order to investigate what gradient results would be obtained if different sets of distances from the literature were selected for given clusters, we recalculated the oxygen gradients in a few cases. We concentrated on those objects for which there were the largest discrepancies in the distances found in the literature: we tested all different distance estimates available for NGC 6204, NGC 6604, Vul OB1, NGC 4755, and Cep OB2 and verified that the gradients do not change significantly. We also adopted different distances for NGC 1893 and the H II regions Sh2 247 and Sh2 285. For these, if, for example, the smallest distance estimates of 3.6 kpc, 2.2 kpc and 4.3 kpc, respectively, were adopted, the oxygen gradient would be $-0.034 \text{dex kpc}^{-1}$. On the other hand, the oxygen gradient would flatten to $-0.028 \text{dex kpc}^{-1}$ if we had considered them to be further away from the Sun having $d=6.0$, 3.5 kpc and 6.9 kpc, respectively. Although these two slopes are different, it is reassuring that they are within the estimated uncertainty for the oxygen gradient quoted in Table 3 ($\sigma b=0.012 \text{ dex kpc}^{-1}$).

5.1. Comparisons with Published Gradients

A summary of the metallicity gradients obtained by recent studies of early-type stars starts with the work by Gummersbach et al. (1998). They analyzed 16 stars belonging to 11 clusters or OB associations with Galactocentric distances between $5.6 < R_g < 13.5$ kpc: ten stars with $R_g > 8$ kpc are from the sample of Kaufer et al. (1994, who originally found an almost null gradient for nitrogen and oxygen); plus six additional stars from the inner disk ($R_g < 8$ kpc). Non-LTE abundances were derived self-consistently and their resulting gradients are: -0.035 ± 0.014 dex kpc $^{-1}$ for carbon, -0.078 ± 0.023 dex kpc $^{-1}$ for nitrogen, -0.067 ± 0.024 dex kpc $^{-1}$ for oxygen, -0.082 ± 0.026 dex kpc $^{-1}$ for magnesium, -0.045 ± 0.023 dex kpc $^{-1}$ for aluminum and -0.107 ± 0.028 dex kpc $^{-1}$ for silicon. In general, these gradients are steeper than the slopes of abundance with Galactocentric distances derived in this study (listed in Table 3); although, for carbon and aluminum the gradients in both studies are comparable.

A few comments can be made about the Gummersbach et al. (1998) sample and derived gradients. The latter are quite dependent on the star Sh2 217-3, which lies ~ 13 kpc from the Galactic center. For oxygen, in particular, if this star is discarded and the oxygen gradient is recomputed for their fifteen remaining stars, a shallower slope (by a factor of two) of -0.035 ± 0.024 dex kpc $^{-1}$ is derived. Such a dependence on the abundance of one star is understandable because their sample is relatively small and more weighted towards smaller Galactocentric distances (fifteen out of sixteen targets have $R_g < 12$ kpc). Five stars in their sample belong to the Orion OB1 association, which is located 500 parsecs away from the Sun in the direction of the anticenter. The oxygen abundance results in Gummersbach et al. (1998) for the Orion targets span a range of $\Delta(O)=0.63$ dex (taken to be the difference between the largest and smallest oxygen abundance). It is interesting to note that a similar range in oxygen abundance is found when considering Gummersbach et al.'s whole sample, that covers a large interval in Galactocentric positions: $\Delta(O) = 0.59$ dex. If these oxygen abundance results are in fact representative of the abundance distribution of OB stars in the Galactic disk, one possible interpretation is that the Orion association was able to produce, internally, the same observed range in oxygen abundances as that encompassed by the radial distribution along roughly 7 kpc of the Galactic disk. This is supported by the discussion in Cunha & Lambert (1994) who observed a similar spread in oxygen abundances for Orion that could not be easily explained from the expected uncertainties in the analysis and suggested that a process of self-enrichment by nucleosynthesis products of Supernovae type II might have happened in Orion in short timescales.

A large abundance database of OB stars within Galactocentric distances $R_g=6.1$ and 13.2 kpc has been built over the years 1983 – 1994 by the Irish group. Their abundance

data were later extended to larger Galactocentric radii by Smartt, Dufton, & Rolleston (1996a,b,c). This stellar sample, combined with the former, was studied by Smartt & Rolleston (1997) who derived oxygen abundances in non-LTE from tabulated theoretical equivalent widths of O II lines published by Becker & Butler (1988). As discussed in Cunha & Lambert (1994), these published non-LTE calculations used inadequately blanketed model atmospheres by Gold (1984). More recently, the observational data (stellar parameters, distances and equivalent widths) from the Irish group were compiled by Rolleston et al. (2000). They recomputed the abundances in LTE and obtained an oxygen gradient of $-0.067 \pm 0.008 \text{ dex kpc}^{-1}$, for 72 stars at 22 disk positions between $R_g=6.06$ and 17.6 kpc. Their derived gradients for C, N, Mg, Al, and Si were all roughly similar in magnitude: the average gradient for the six elements analyzed being $-0.068 \pm 0.013 \text{ dex kpc}^{-1}$. Their gradients are considerably steeper than the slopes obtained here from our sample. It can be argued, however, that given the differences in the techniques adopted in the original studies from which Rolleston et al. (2000) collected their measurements (equivalent widths for different line sets, and stellar parameters derived non-homogeneously), it is possible that different systematic errors (e.g. in the T_{eff} —scale, microturbulence, and line sets) may be affecting their absolute abundances, as well as the final gradients. Moreover, as recognized in Rolleston et al. (2000), the adoption of a fully self-consistent non-LTE approach would result in abundances that are expected to be more accurate on an absolute scale, even if they conclude in their study that the LTE approach will not influence the metallicity gradients themselves.

The inner parts of the disk were studied by Smartt et al. (2001). They analyzed four B stars within 2.5–5 kpc of the Galactic center and found LTE oxygen abundances close to solar (considering our adopted value of 8.66) for two of them, while the other two stars showed overabundances of oxygen relative to the Sun of roughly 0.4 dex. These abundance results do not seem consistent with what would be expected from a simple extrapolation, towards smaller Galactocentric distances, of the steep oxygen gradient obtained by Rolleston et al. (2000), which would lead to oxygen abundances around 9.2–9.3 dex. On the other hand, however, for C, N, Mg, Al, and Si, they find enhanced abundances that are roughly in agreement with an extrapolation of steep metallicity gradients.

As discussed before, the most internal and external parts of the Galactic disk are not probed in our study. An extension of our sample would be desirable and is possible with the inclusion of additional targets from other literature studies. In order to investigate what effects the addition of these targets would have on our derived gradients, we attempted to analyze them using the same methodology adopted for our sample stars (although not via a fully self-consistent analysis because we do not have the observed spectra). The abundances were not directly taken from the literature, but were analyzed as follows: we used the Q-

calibration in order to derive new effective temperatures for the stars and adopted their surface gravities from the literature. We then calculated non-LTE profiles of O II lines that reproduced their published equivalent widths. The Galactocentric distances were also recalculated for $R_\odot = 7.9\text{ kpc}$, using the mean distances from the literature, when more than one distance determination was available. We reanalyzed 10 stars, at 9 new positions in the disk: star Sh2 217-3, the farthest star and with the lowest abundance in the sample of Gummersbach et al. (1998); the most distant stars in Rolleston et al. (2000), namely RLWT 13, RLWT 41, Sh2 208-6, Sh2 289-2, Sh2 289-4 and Sh2 283-2; and three stars of Smartt et al. (2001), located in the inner parts of the Galactic disk. These stars were then combined with our sample, yielding a new gradient of $-0.045 \pm 0.010 \text{ dex kpc}^{-1}$ for oxygen, in the range 2.7–16.0 kpc. The change in the slope marginally exceeds the expected errors, however, it is not large enough to make it comparable to a steeper gradient of $\sim -0.07 \text{ dex kpc}^{-1}$. This suggests that our flatter gradients are not the result of the sample of OB stars that were analyzed.

5.2. Gradients from Galactic Chemical Evolution Models

Radial gradients are important large-scale observational constraints for models of chemical evolution of the Galaxy. The disk metallicity gradients in this study were inferred from the photospheric abundances of young OB stars, assuming that these abundances represent the composition of the gas from which they formed.

5.2.1. *Are the Abundances of OB Stars Representative of Their Natal Clouds?*

Before comparing our results for OB stars with chemical evolution models that describe the evolution of the gas with Galactocentric distance, we will discuss briefly if it seems reasonable to use abundances in OB stars to trace the metallicity distribution of the Galactic disk. This assumption has been questioned in Sofia & Meyer (2001), based in part on the fact that there was a discrepancy between the abundances of OB stars and the higher solar abundances used as comparison at that time. To solve this discrepancy, they follow Snow (2000) and suggest a mechanism to reject heavy elements during star formation, producing the lower heavy-element B-star abundances. Such mechanisms as proposed by Snow (2000) are processes of sedimentation of refractory elements onto dust grains (and thus decoupled from the gas) and/or ambipolar diffusion of charged dust grains by magnetic fields. The situation has changed with the most recent, and lower, solar abundance determinations for C, N, and O from 3-D model atmospheres by Asplund (2003) and Asplund et al. (2004)

that bring the abundances of OB stars and the Sun into a general agreement (see review by Herrero 2003). In particular, for our abundance database (as pointed out in Paper VI) the revised solar oxygen abundance falls roughly at the peak of the abundance distribution of our 60 sample OB stars from the inner Galactic disk (see histogram in Figure 2 of Paper VI), while the abundances of outer disk B stars are on average lower.

However, even if abundance discrepancies between B stars and the Sun are probably resolved, the physical processes that may affect the abundances in the atmospheres of these hot stars need to be investigated in detail. The indications that diffusion processes actually take place in these stellar atmospheres seem weakened. Quiet atmospheres are a requirement for diffusion to occur. However, OB stars are usually fast rotators (even stars with low $v \sin i$ may be fast-rotators seen pole-on); in addition, the microturbulent velocities derived from non-LTE analysis of OB stars are typically non-zero and sometimes found to be around 10 km s^{-1} (Gies & Lambert 1992; Mathys et al. 2002). Therefore, it is expected that the velocity fields produced by rotation and microturbulence in the outer layers of the atmospheres of OB stars may lead to mixing and thus inhibit diffusion (Morel & Thévenin 2002; Hempel & Holweger 2003).

5.2.2. Comparisons with Chemical Evolution Models

Several Galactic chemical evolution models are available in the literature and these seek to reproduce observed trends of abundance with Galactocentric distance in the Milky Way disk. In Figure 6 we show the abundances obtained for our studied clusters and OB associations compared to curves that represent the theoretical radial gradients predicted by three different models that assume inside-out formation of the disk, i.e., assume differing timescales for inner and outer disk formation, with the inner disk having formed first.

Hou, Prantzos, & Boissier (2000) assume infall of external material and a multi-slope power-law IMF, with no density threshold for the star formation in the disk. In addition, they deliberately neglected the yields from intermediate mass stars in their models, which led them to conclude that most of abundance distributions, except for C and N (not shown in Figure 6), could be reproduced using only the yields of massive stars. The model of Alibés, Labay, & Canal (2001b) is an extension of their previous chemical evolution model for the solar neighbourhood (Alibés, Labay, & Canal 2001a) and also assumes a multi-slope power-law IMF and infall, with two different compositions for the infalling matter: primordial and enriched. The radial gradients calculated for enriched infalling matter are slightly flatter than those predicted assuming primordial infalling material: the oxygen gradients are -0.047 and $-0.053 \text{ dex kpc}^{-1}$, respectively. These gradients are steeper than the oxygen gradient

obtained from our sample. The gradients calculated for the other elements are also steeper than ours and agree only marginally considering the uncertainties. Chiappini, Matteucci, & Romano (2001) considered four different scenarios in their models of Galactic chemical evolution, by basically changing the halo evolution. One of their models (model B) gives the flattest slopes, with the oxygen gradient being in good agreement with the gradient derived in this study. On the other hand, steeper gradients, consistent with a gradient of $-0.07 \text{ dex kpc}^{-1}$, can be obtained with their models A and C (models A and C are similar except that model C assumes no threshold in the gas density during the halo/thick disk-phase). The differences between the models A, B, and C (the adopted halo mass density profiles and the density thresholds in the halo phase) suggest that the differences in the history of the halo evolution affect mainly the outer gradients ($R_g > 10 \text{ kpc}$) whereas the inner gradients are unchanged.

A simple inspection of the C, N and O panels of Figure 6 indicates that it seems that all sets of models attempted to reproduce previous (and higher) solar abundances; the adoption now of lower solar abundances of CNO produces the observed discrepancies between the models and the Sun. [We recall that we consider the lower values of Asplund (2003); Asplund et al. (2004) for CNO]. The same applies to the comparison between the models and abundances of OB stars; it seems clear that the predicted gradients for C, N, O, Al and Si fall above the observed abundances, especially in the inner parts of the disk. For oxygen, in particular, it is interesting to point out again the significantly lower abundances obtained for all three studied objects in our sample with Galactocentric distances between roughly $R_g = 9$ and 11 kpc . This apparent drop in the oxygen abundance (if real) is not mimicked by any model; even if we were allowed to simply slide all the model curves downwards in order to fit the Sun. The predicted gradients for Mg are also higher than the observed abundances, but the discrepancy, in this case, is less pronounced. For sulfur, however, there seems to be good agreement between the observations (derived abundances) with model B from Chiappini, Matteucci, & Romano (2001).

5.3. Time Evolution of the Abundance Gradients

The variation of the radial gradients as a function of time is predicted by model calculations and also is suggested from observations. The models by Hou, Prantzos, & Boissier (2000) and Alibés, Labay, & Canal (2001b) predict a flattening of the radial gradients with time. Observational indication that the gradients flatten with time was presented in Friel et al. (2002) and also in Chen, Hou, & Wang (2003), based on analyses of open cluster metallicities. In these studies, the gradients obtained from clusters in their youngest age bracket

were always flatter than those derived for the older clusters. Maciel, Costa & Uchida (2003) obtained essentially the same results using planetary nebulae having progenitor stars with different masses and ages.

The flattening of the gradients is generally measured over Gyr timescales, whereas our sample of young OB stars – 19 out of 26 clusters have ages below 10 Myr (Dias et al 2002) – represents in principle the present time composition of the Galactic disk; they span a relatively narrow age interval and are not best suited to evaluate time variations of the radial gradients. However, if we simply segregate from our sample those clusters younger than 10 Myr, we obtain gradients that are fully consistent with those gradients derived for the whole sample and listed in Table 3. The seven clusters of our sample older than 10 Myr are concentrated in the region between 6-8 Kpc away from the Galactic center. A meaningful gradient cannot, therefore, be computed for this older sample.

It is of interest, however, to compare the present-day gradients we derived from young OB stars with the time evolution of metallicity gradients inferred from observations of objects that span a larger age interval. This is shown in Figure 7, where we plot our average slope of $-0.042 \text{ dex kpc}^{-1}$, representing the present-day radial metallicity gradient, and the metallicity gradients inferred from open clusters and PNe with different ages. The clusters [Fe/H] gradients are from Friel et al. (2002); Chen, Hou, & Wang (2003) and the age bins are represented in the figure by a mean age plus dispersion (horizontal errorbars), computed directly from their published data. We also show the evolution of the [Fe/H] gradients inferred from the oxygen gradients of Maciel, Costa & Uchida (2003), adopting the $[\text{Fe}/\text{H}] \times [\text{O}/\text{H}]$ relation presented in their paper. For the PNe ages, usually subject to large uncertainties, we adopted simply the middle value of each age bin (0–4, 4–5 and > 5 Gyr) and the errorbars represent the typical uncertainties assigned to their adopted ages. An inspection of this figure indicates that the flatter gradients derived for OB stars in this study are quite consistent with a general flattening of the radial gradients with time.

6. Conclusions

We have studied the distribution of metallicity with Galactocentric distance for a large sample of main-sequence OB stellar members of clusters and associations in the Galactic disk. A uniform methodology was adopted resulting in a homogeneous database of non-LTE abundances of the elements carbon, nitrogen, oxygen, magnesium, aluminum, silicon and sulfur that can be used to constrain chemical evolution models. The radial gradients derived from this abundance database are flatter than the recent results for early-B stars. The slope averaged from all elements is found to be $-0.042 \pm 0.007 \text{ dex kpc}^{-1}$ and the oxygen gradient,

in particular, is $-0.031 \text{ dex kpc}^{-1}$.

These flatter gradients are in agreement with the most recent nebular abundances from H II regions and PNe that find flatter oxygen gradients for the Galactic disk (Deharveng, Peña, & Caplan 2000; Pilyugin, Ferrini, & Shkvarun 2003; Henry, Kwitter & Balick 2004) and are in line with the expected flat gradient caused from the presence of a bar in the Galactic center (Bissantz & Gerhard 2002; Weiner & Sellwood 1999). Furthermore, an extension of the obtained metallicity gradients to the Galactic center is consistent with the mean metallicity derived by Ramírez et al. (2000) for a sample of evolved stars located within 2.5 pc from the Galactic center, $[\text{Fe}/\text{H}] = +0.12 \pm 0.22$. Near solar oxygen abundances were also found by Smartt et al. (2001) and Munn et al. (2004) for a sample of early B-stars in the innermost Galactic disk, favouring a flat oxygen gradient towards the Galactic center. Our average slope is also consistent with a flattening of the radial gradients as a function of time, predicted by models and also supported by observational evidences based on abundances in open clusters and PNe. The derived gradients are believed to be a solid representation of the behavior of abundance with Galactocentric distances within 5 to 13 kpc from the Galactic center.

We would like to thank Dr. Cristina Chiappini for nice discussions.

REFERENCES

Afflerbach, A., Churchwell, E. & Werner, M. W. 1997, *ApJ* 478, 190

Alibés, A., Labay, J., & Canal, R. 2001a, *A&A* 370, 1103

Alibés, A., Labay, J., & Canal, R. 2001b, *astro-ph/0107016*

Allen, C., Carigi, L., & Peimbert, M. 1998, *ApJ* 494, 247

Alter, G., Balazs, B., & Ruprecht, J. 1970, in ‘Catalogue of Star Clusters and Associations’ (Hungary: Akadémiai Kiadó Budapest)

Andrievsky, S. M., Luck, R. E., Martin, P., & Lépine, J. R. D. 2004, *A&A* 413, 159

Asplund, M. 2003, in CNO in the Universe, *ASP Conference Series* 304, ed. C. Charbonnel, D. Schaerer and G. Meynet (San Francisco: ASP), 275

Asplund, N., Grevesse, N., Sauval, A.J., Allende Prieto, C. & Kiselman, D. 2004, *A&A* 417, 751

Becker, S. R. & Butler, K. 1988, *A&A* 201, 232

Becker, W. & Fenkart, R. 1971, *A&AS* 4, 241

Bissantz, N. & Gerhard, O. 2002, *MNRAS* 330, 591

Blitz, L., Fich, M., & Stark, A. A. 1982, *ApJS* 49, 183

Caputo, F., Marconi, M., Musella, I., & Pont, F. 2001, *A&A* 372, 544

Chen, L., Hou, J. L., & Wang, J. J. 2003, *AJ* 125, 1397

Chiappini, C., Matteucci, F., & Romano, D. 2001, *ApJ* 554, 1044

Crampton, D. L. 1971, *AJ* 76, 260

Crampton, D. L., Georgelin, Y. M., & Georgelin, Y. P. 1978, *A&A* 66, 1

Crawford, D. L., Barnes, J. V., Hill, G., & Perry, C. L. 1971, *AJ* 76, 1048

Cuffey, J. 1973, *AJ* 78, 747

Cunha, K. & Lambert, D. L. 1994, *ApJ* 426, 170

Daflon, S., Cunha, K., & Becker, S. 1999, *ApJ* 522, 950 (Paper I)

Daflon, S., Cunha, K., Becker, S., & Smith, V. V. 2001a, *ApJ* 552, 309 (Paper II)

Daflon, S., Cunha, K., Butler, K., & Smith, V. V. 2001b, *ApJ* 563, 325 (Paper III)

Daflon, S., Cunha, K., Smith, V. V., & Butler, K. 2003, *A&A* 399, 525 (Paper IV)

Daflon, S., Cunha, K., & Butler, K. 2004a, *ApJ* 604, 362 (Paper V)

Daflon, S., Cunha, K., & Butler, K. 2004b, *ApJ* 606, 514 (Paper VI)

Deharveng, L., Peña, M., Caplan, J., & Costero, R. 2000, *MNRAS* 311, 329

de Zeeuw, P. T., Hoogerwerf, R., de Bruijne, J. H. J., Brown, A. G. A., & Blaauw, A. 1999, *AJ* 117, 354

Dias, W. S., Alessi, B. S., Moitinho, A. & Lépine, J. R. D. 2002, *A&A* 389, 871

Feinstein, A. 1994, *Rev. Mex. Astron. y Astrof.* 29, 141

Fitzgerald, M. P. & Moffat, A. F. J. 1980, *MNRAS* 193, 761

Fitzsimmons, A. 1993, *A&AS* 99, 15

Fitzsimmons, A., Brown, P. J. F., Dufton, P. L., & Lennon, D. J. 1990, *A&A* 232, 437

Friel, E. D., Janes, K. A., Tavarez, M., Scott, J., Katsanis, R., Lotz, J., Hong, L., & Miller, N. 2002, *AJ* 124, 2693

Georgelin, Y. M. & Georgelin, Y. P. 1976, *A&A* 49, 57

Gies, D. R. & Lambert, D. L. 1992, *ApJ* 387, 673

Gold, M. 1984, Diplomarbeit, Ludwig Maximilian Universität

Grevesse, N. & Sauval, A. J. 1998, *Space Sci. Rev.* 85, 161

Gummersbach, C. A., Kaufer, A., Schäfer, D. R., Szeifert, T., & Wolf, B. 1998, *A&A* 338, 881

Han, J. L., Manchester, R. N., Lyne, A. G., & Qiao, G. J. 2002, *ApJ* 570, L17

Heger, A., & Langer, N. 2000, *ApJ*, 544, 1016

Hempel, M. & Holweger, H. 2003, *A&A* 408, 1065

Henry, R. B. C. & Worthey, G. 1999, *PASP* 111, 919

Henry, R. B. C., Kwitter, K. B. & Balick, B. 2004, AJ 127, 2284

Herrero, A. 2003, in CNO in the Universe, ASP Conference Series 304, ed. C. Charbonnel, D. Schaerer and G. Meynet (San Francisco: ASP), 10

Holweger, H. 2001, in Solar and Galactic Composition, ed. R. F. Wimmer-Schweingruber (American Institute of physics), p. 23

Hou, J. L., Prantzos, N., & Boissier, S. 2000, A&A 362, 921

Humphreys, R. M. 1978, ApJ 38, 309

Humphreys, R. M. & McElroy, D.B. 1984, in ‘Catalogue of Stars in Stellar Associations and Young Clusters’, Univ. of Minnesota

Kaltcheva, N. T. & Georgiev, L. N. 1992, MNRAS 259, 166

Kaufer, A., Szeifert, Th., Krenzin, R., Baschek, B., & Wolf, B. 1994, A&A 289, 740

Kennicutt, R. C., Bresolin, F. & Garnett, D. R. 2003, ApJ, 591, 801

Kilian-Montenbruck, J., Gehren, T., & Nissen, P. E. 1994, A&A 291, 757

Lahulla, J. F. 1985, A&AS 61, 537

Lahulla, J. F. 1987, AJ 94, 1062

Lennon, D. J., Dufton, P. L. , Fitzsimmons, A., Gehren, T., & Nissen, P. E. 1990, A&A 240, 349

MacNamara, D. H., Madsen, J. B., Barnes, J., & Erickson, B. F. 2000, PASP 112, 202

Maciel, W. J. & Quireza, C. 1999, A&A 345, 629

Maciel, W. J., Costa, R. D. D. & Uchida, M. M. M. 2003, A&A 397, 667

Marco, A., Bernabeu, G., & Negueruela, I. 2001, AJ 121, 2075

Martin, P. & Roy, J.-R. 1994, ApJ 424, 599

Martins, L. P. & Viegas, S. M. M. 2000, A&A 361, 1121

Mathys, G., Andrievsky, S. M., Barbuy, B., Cunha, K., & Korotin, S. A. 2002, A&A 387, 890

Mel’nik, A.M. & Efremov, Yu.N. 1995, PAZh 21, 13

Moffat, A. F. J., Fitzgerald, M. P., & Jackson, P. D. 1977, *ApJ* 215, 106

Moffat, A. F. J., Fitzgerald, M. P., & Jackson, P. D. 1979, *A&AS* 38, 197

Moffat, A. F. J. & Vogt, N. 1975a, *A&AS* 20, 155

Moffat, A. F. J. & Vogt, N. 1975b, *A&AS* 20, 85

Monteverde, M. I., Herrero, A., Lennon, D. J., & Kudritzki, R.-P. 1997, *ApJ* 474, L107

Morel, P. & Thévenin, F. 2002, *A&A* 390, 611

Munn, K. E., Dufton, P. L., Smartt, S. J., & Hambly, N. C. 2004, *A&A* 419, 713

Pérez, M. R., Thé, P. S., & Werterlund, B. E. 1987, *PASP* 99, 1050

Pilyugin, L.S., Ferrini, F., & Shkvarun, R. V. 2003, *A&A* 401, 557

Ramírez, S. V., Sellgren, K., Carr, J. S., Balachandran, S. C., Blum, R., Terndrup, D. M., & Steed, A. 2000, *ApJ* 537, 205

Reichen, M., Lanz, T., Golay, M., & Huguenin, D. 1990, *Ap&SS* 163, 275

Reid, M. J. 1993, *ARA&A* 31, 345

Rolleston, W. R. J., Dufton, P. L., & Fitzsimmons, A. 1994, *A&A* 284, 72

Rolleston, W. R. J., Smartt, S. J., Dufton, P. L., & Ryans, R. S. I. 2000, *A&A* 363, 537

Sagar, R. & Joshi, U. C. 1981, *Ap&SS* 75, 465

Shaver, P.A., McGee, R.X., Newton, M.P., Danks, A.C., & Pottasch, S.R. 1983, *MNRAS* 204, 53

Shobbrook, R. R. 1984, *MNRAS* 206, 273

Sofia, U. J. & Meyer, D. M. 2001, *ApJ* 554, L221

Smartt, S. J., Dufton, P. L., & Rolleston, W. R. J. 1996a, *A&A* 305, 164

Smartt, S. J., Dufton, P. L., & Rolleston, W. R. J. 1996b, *A&AS* 116, 483

Smartt, S. J., Dufton, P. L., & Rolleston, W. R. J. 1996c, *A&A* 310, 123

Smartt, S. J. & Rolleston, W. R. J. 1997, *ApJ* 481, L47

Smartt, S. J., Venn, K. A., Dufton, P. L., Lennon, D. J., Rolleston, W. R. J., & Keenan, F. P. 2001, A&A 367, 86

Snow, T. P. 2000, Journal of Geophys. Research 105, A5 1023

Tapia, M., Costero, R., Echevarría, J., & Roth, M. 1991, MNRAS 253, 649

Tovmassian, H. M., Epremian, R. A., Kovhannesian, R. Kh., Cruz-Gonzalez, G., Navarro, S. G., & Karapetian, A. A. 1998, AJ 115, 1083

Turbide, L. & Moffat, A. F. J. 1993, AJ 105, 1831

Twarog, B. A., Ashman, K. M., & Anthony-Twarog, B. J. 1997, AJ 114, 2556

van der Hucht, K. A., Thé, P. S., & Bakker, R. 1980, PASP 92, 837

Vila-Costas, M. B. & Edmunds, M. G. 1992, MNRAS 259, 121

Vílchez, J. M. & Esteban, C. 1996, MNRAS 280, 720

Vogt, N. & Moffat, A. F. J. 1975, A&A 45, 405

Weiner, B. J. & Sellwood, J. A. 1999, ApJ 524, 112

Table 1. Cluster Abundances

Object	$\log \epsilon(\text{C})[\text{n}]$	$\log \epsilon(\text{N})[\text{n}]$	$\log \epsilon(\text{O})[\text{n}]$	$\log \epsilon(\text{Mg})[\text{n}]$	$\log \epsilon(\text{Al})[\text{n}]$	$\log \epsilon(\text{Si})[\text{n}]$	$\log \epsilon(\text{S})[\text{n}]$
Sh2 47	8.21[1]	7.53[1]	8.52[1]	7.48[1]	6.32[1]	7.40[1]	7.15[1]
NGC 6611	8.25 \pm 0.20[2]	7.61 \pm 0.09[4]	8.58 \pm 0.07[4]	7.41 \pm 0.12[4]	6.11 \pm 0.24[3]	7.16 \pm 0.21[4]	7.21 \pm 0.10[3]
Sh2 32	8.26[1]	7.73 \pm 0.06[2]	8.66 \pm 0.09[2]	7.55[1]	6.34[1]	7.30 \pm 0.13[2]	7.30[1]
NGC 6204	8.12[1]	7.72[1]	8.68[1]	7.32[1]	6.10[1]	7.57[1]	...
Trumpler 27	8.45[1]	7.81[1]	8.55 \pm 0.04[2]	7.80[1]	6.30[1]	7.48 \pm 0.06[2]	7.47[1]
NGC 6231	8.20 \pm 0.12[4]	7.63 \pm 0.20[4]	8.52 \pm 0.05[4]	7.34 \pm 0.16[3]	5.98 \pm 0.18[4]	7.14 \pm 0.23[4]	7.19 \pm 0.03[4]
NGC 6604	...	7.55[1]	8.53[1]	7.57[1]	6.10[1]	7.20[1]	...
Ara OB1	8.29[1]	7.55[1]	8.58[1]	7.57[1]	6.12[1]	7.20[1]	7.21[1]
Vul OB1	...	7.77 \pm 0.33[2]	8.46 \pm 0.25[2]	7.45 \pm 0.20[2]	6.09 \pm 0.20[2]	7.44 \pm 0.08[2]	7.20 \pm 0.11[2]
Stock 16	8.49[1]	7.77[1]	8.50[1]	7.22[1]	6.11[1]	7.09[1]	7.30[1]
Sct OB2	8.30 \pm 0.06[2]	7.59 \pm 0.10[2]	8.54 \pm 0.05[2]	7.73 \pm 0.04[2]	6.33 \pm 0.14[2]	7.72 \pm 0.04[2]	7.45[1]
NGC 4755	8.26 \pm 0.05[3]	7.61 \pm 0.10[3]	8.58 \pm 0.05[4]	7.49 \pm 0.21[4]	6.15 \pm 0.15[2]	7.08 \pm 0.06[4]	7.28 \pm 0.09[3]
IC 2944	8.32[1]	7.47 \pm 0.05[2]	8.55 \pm 0.06[2]	7.46 \pm 0.10[2]	5.99 \pm 0.30[2]	7.15 \pm 0.01[2]	7.41[1]
Cyg OB3	8.15 \pm 0.23[2]	7.60 \pm 0.15[4]	8.58 \pm 0.12[5]	7.46 \pm 0.24[4]	6.08 \pm 0.21[4]	7.38 \pm 0.17[5]	7.26 \pm 0.07[3]
Cyg OB7	8.05[1]	7.83 \pm 0.26[3]	8.69 \pm 0.20[3]	7.36 \pm 0.02[2]	6.07 \pm 0.18[2]	7.15 \pm 0.09[3]	7.11[1]
Lac OB1	8.36 \pm 0.02[3]	7.68 \pm 0.11[5]	8.67 \pm 0.16[5]	7.51 \pm 0.04[3]	6.13 \pm 0.11[4]	7.26 \pm 0.20[5]	7.19 \pm 0.11[4]
Cep OB2	8.17 \pm 0.09[5]	7.57 \pm 0.14[17]	8.53 \pm 0.14[17]	7.38 \pm 0.18[16]	5.98 \pm 0.18[16]	7.25 \pm 0.30[17]	7.20 \pm 0.10[6]
Cep OB3	...	7.56 \pm 0.06[2]	8.54 \pm 0.13[3]	7.20 \pm 0.21[3]	5.87 \pm 0.14[3]	7.09 \pm 0.18[3]	7.14 \pm 0.07[3]
Ori OB1*	8.39 \pm 0.11[15]	7.76 \pm 0.13[15]	8.72 \pm 0.13[18]	7.13 \pm 0.13[18]	...
Mon OB2	...	7.19[1]	8.08[1]	6.86[1]	5.91[1]	7.08[1]	6.94[1]
Sh2 247	...	7.40[1]	8.20[1]	7.28[1]	...	7.34[1]	...
NGC 2414	8.00[1]	7.28 \pm 0.13[2]	8.08 \pm 0.07[2]	7.13[1]	5.99[1]	6.63 \pm 0.03[2]	...
Sh2 253	8.05[1]	7.45[1]	8.55[1]	6.98[1]	5.92[1]	7.00[1]	...
NGC 1893	8.03[1]	7.31 \pm 0.01[2]	8.37 \pm 0.05[2]	7.16[1]	5.79[1]	6.79 \pm 0.01[2]	7.02[1]
Sh2 284	7.98[1]	7.39[1]	8.46[1]	7.25[1]	5.68[1]	7.30[1]	7.08[1]
Sh2 285	8.08[1]	7.45[1]	8.49[1]	7.32[1]	6.04[1]	7.29[1]	6.95[1]

*non-LTE abundances from Cunha & Lambert (1994).

Table 2. Cluster Distances

Cluster	$l(^{\circ})$	$b(^{\circ})$	d (kpc)	$\langle d \rangle$ (kpc)	R_g (kpc)
Sh2 47	15.3	0.1	$3.7^1, 3.1^2$	3.4 ± 0.4	4.7 ± 0.5
NGC 6611	17.0	0.8	$2.19^3, 2.5^4, 2.6^5, 1.68^6$	2.2 ± 0.4	5.8 ± 0.5
Sh2 32	7.3	−2.0	$1.8^8, 2.2^9$	2.0 ± 0.3	5.9 ± 0.4
NGC 6204	338.3	−1.1	$2.51^3, 2.6^4, 1.32^6, 1.94^7$	2.1 ± 0.6	6.0 ± 0.6
Trumpler 27	355.1	−0.7	$2.0^5, 1.65^{11}, 2.1^{32}$	1.9 ± 0.2	6.0 ± 0.3
NGC 6231	343.5	1.2	$1.8^4, 1.6^5, 1.77^6, 2.0^{10}$	1.8 ± 0.2	6.2 ± 0.3
NGC 6604	18.3	1.7	$0.70^4, 2.1^5, 1.64^{12}$	1.5 ± 0.7	6.5 ± 0.7
Ara OB1	336.3	−1.4	$1.38^3, 1.4^6, 1.59^7, 1.1^{13}$	1.4 ± 0.2	6.6 ± 0.3
Vul OB1	59.4	−0.1	$2.0^3, 2.54^7, 3.5^{17}$	2.7 ± 0.7	6.9 ± 0.3
Stock 16	306.1	0.1	$1.9^5, 2.0^{14}$	1.9 ± 0.1	6.9 ± 0.3
Sct OB2	39.0	7.6	$1.0^3, 1.17^{15}$	1.1 ± 0.1	7.1 ± 0.3
NGC 4755	303.2	2.5	$2.34^4, 1.03^6, 1.9^{16}$	1.8 ± 0.7	7.1 ± 0.4
IC 2944	294.6	−1.4	$2.1^4, 2.0^5, 1.95^6, 2.2^{18}$	2.1 ± 0.1	7.3 ± 0.3
Cyg OB3	73.5	2.0	$2.29^3, 1.9^5, 2.31^7$	2.2 ± 0.2	7.6 ± 0.3
Cyg OB7	90.0	2.0	$0.83^3, 0.79^{21}$	0.8 ± 0.1	7.9 ± 0.3
Lac OB1	96.8	−16.1	$0.6^3, 0.63^7, 0.368^{19}$	0.6 ± 0.1	8.0 ± 0.3
Cep OB2	99.2	3.8	$0.83^3, 0.95^5, 0.96^7, 0.615^{19}$	0.8 ± 0.2	8.1 ± 0.3
Cep OB3	110.4	2.8	$0.87^3, 0.725^6, 0.84^7$	0.8 ± 0.1	8.2 ± 0.3
Ori OB1	205.0	−17.4	$0.5^3, 0.43^4, 0.56^7, 0.438^{19}$	0.5 ± 0.1	8.3 ± 0.3
Mon OB2	206.5	−2.1	$1.51^3, 1.62^6, 1.63^7, 1.67^{20}$	1.6 ± 0.1	9.4 ± 0.3
Sh2 247	188.9	0.8	$3.5^{23}, 2.2^{24}$	2.8 ± 0.9	10.7 ± 0.9
NGC 2414	231.0	2.0	$3.98^{21}, 4.2^{22}$	4.1 ± 0.1	10.9 ± 0.3
Sh2 253/Bo 1	192.4	3.2	$4.4^{23}, 4.8^{27}, 4.06^{29}$	4.4 ± 0.4	12.2 ± 0.5
NGC 1893	173.6	−1.7	$4.0^5, 3.7^6, 3.6^{25}, 4.3^{26}, 4.8^{27}, 6.02^{28}$	4.4 ± 0.9	12.3 ± 0.9
Sh2 284/Do 25	211.9	−1.3	$5.2^{23}, 5.6^{30}, 5.5^{33}$	5.4 ± 0.2	12.8 ± 0.3
Sh2 285	213.9	−0.6	$6.9^{23,30}, 4.3^{31}, 6.4^{24}$	5.9 ± 1.4	13.2 ± 1.3

References. — 1: Crampton, Georgelin, & Georgelin (1978), 2: Lahulla (1985), 3: Humphreys (1978), 4: Alter, Balazs, & Ruprecht (1970), 5: Feinstein (1994), 6: Becker & Fenkart (1971), 7: Mel'nik & Efremov (1995), 8: Blitz, Fich, & Stark (1982), 9: Vogt & Moffat (1975), 10: Crawford et al. (1971), 11: van der Hucht, Thé, & Bakker (1980), 12: Moffat & Vogt (1975a), 13: Kaltcheva & Georgiev (1992), 14: Crampton (1971), 15: Reichen et al. (1990), 16: Shobbrook (1984), 17: Sagar & Joshi (1981), 18: Tovmassian et al. (1998), 19: de Zeeuw et al. (1999), 20: Pérez, Thé, & Werterlund (1987), 21: Humphreys & McElroy (1984), 22: Fitzgerald & Moffat (1980), 23: Moffat, Fitzgerald, & Jackson (1979), 24: Lahulla (1987), 25: Cuffey (1973), 26: Tapia et al. (1991), 27: Fitzsimmons (1993), 28: Marco, Bernabeu & Negueruela (2000), 29: Moffat & Vogt (1975b), 30: Turbide & Moffat (1993), 31: Rolleston, Dufton, & Fitzsimmons (1994), 32: Moffat, Fitzgerald, & Jackson (1977), 33: Lennon et al. (1990)

Table 3. Radial Gradients of Elemental Abundances ($a + bx$)

log(X/H)	a	σa	b	σb	n	R
C	8.513	0.086	-0.037	0.010	21	-0.64
N	7.950	0.093	-0.046	0.011	26	-0.65
O	8.762	0.105	-0.031	0.012	26	-0.46
Mg	7.794	0.121	-0.052	0.014	25	-0.61
Al	6.452	0.085	-0.048	0.010	24	-0.71
Si	7.546	0.147	-0.040	0.017	26	-0.43
S	7.514	0.092	-0.040	0.011	20	-0.64

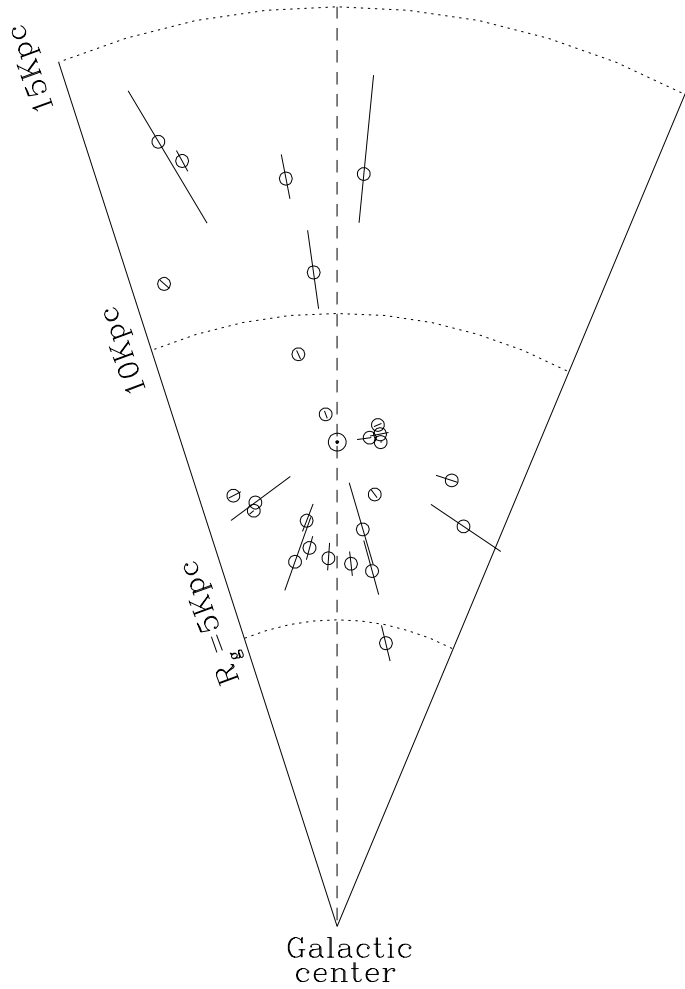


Fig. 1.— The distribution of target clusters and associations projected onto a section of the Galactic Plane. The Sun is represented at $R_{\odot}=7.9$ kpc (MacNamara et al. 2000). The dashed line connects the Sun to the Galactic center and represents the direction $l = 0, 180^\circ$; concentric circles at the distances of 5, 10 and 15 kpc of the Galactic center are depicted by dotted lines. The inclined bars show the range of R_g calculated from different distances in the literature for a given cluster position.

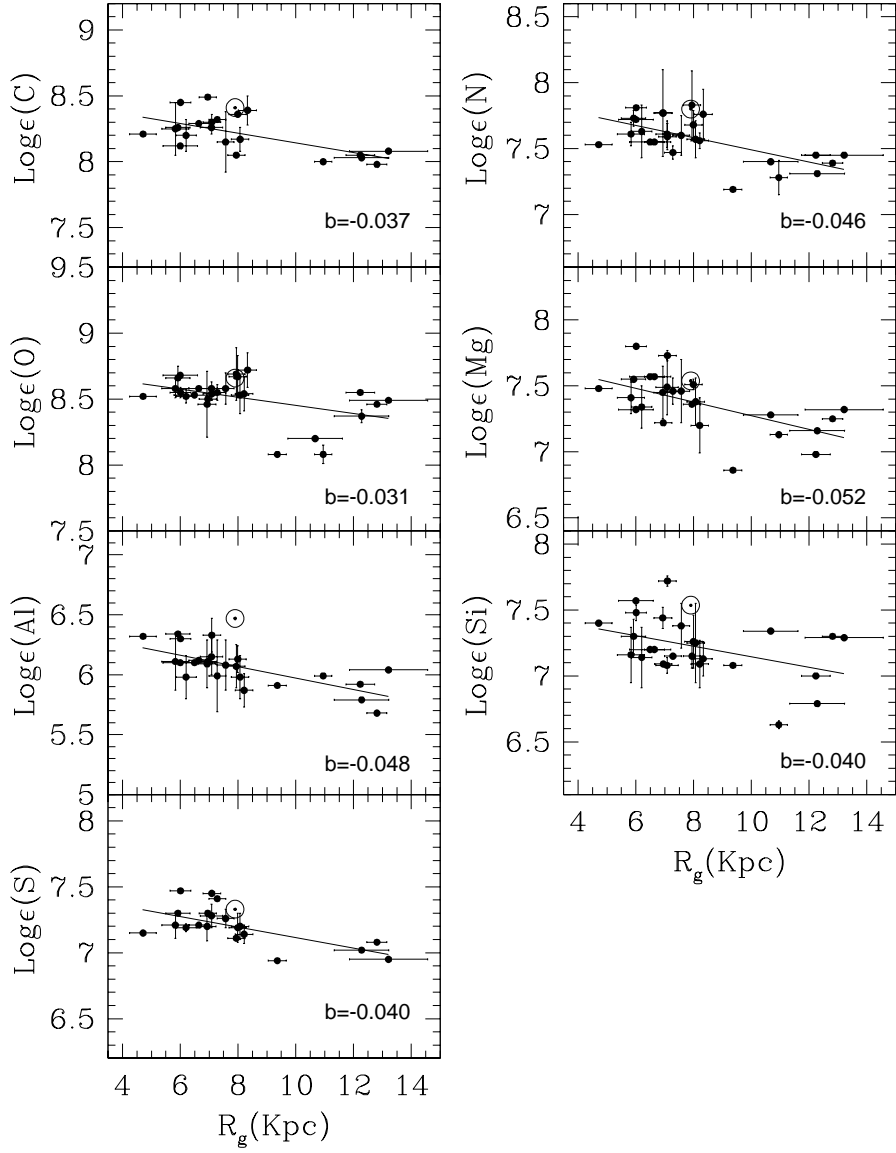


Fig. 2.— Abundance gradients in the Galactic disk derived for C, N, O, Mg, Al, Si and S. The abundances adopted for the clusters are average values of individual stellar abundances in our database. The Sun is at $R_\odot=7.9$ kpc; solar abundances are from Asplund (2003 - C and N), Asplund et al. (2004 - O), Holweger (2001 - Mg and Si), and Grevesse & Sauval (1998 - Al and S).

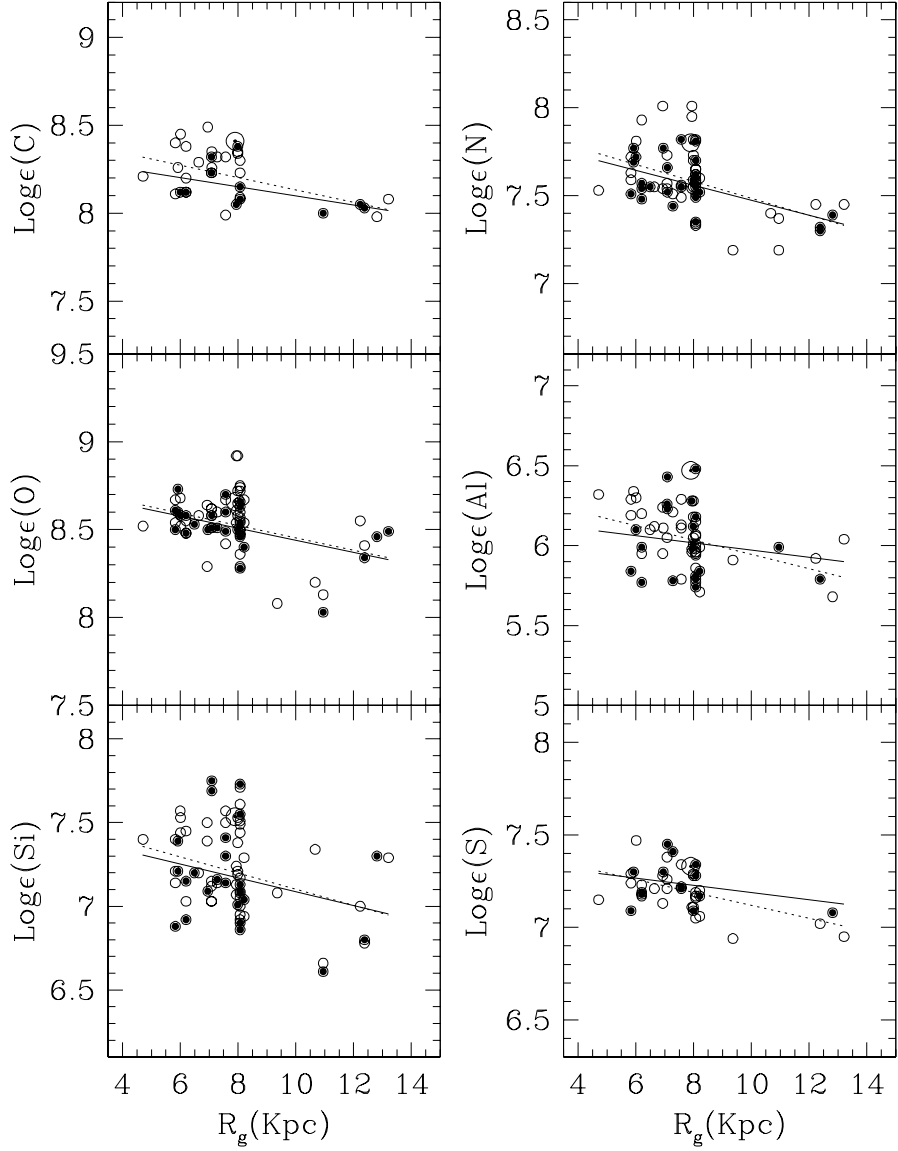


Fig. 3.— A comparison between gradients and stellar abundance distributions for the full sample (open circles, dotted lines) and for the subsample defined according to the maximum line strength temperature, T_{\max} (filled circles, solid lines). From computations of grids of theoretical non-LTE equivalent widths, T_{\max} is reached at approximately: 24 000 K for C II; 26 000 K for N II; 27 500 K for O II; 25 000 K for Al III; 27 000 K for Si III; and 27 000 K for S III. The line strengths of the Mg II triplet at 4481Å reach a maximum at temperatures around 10 000 K; much lower than the lower limit for our OB-star sample.

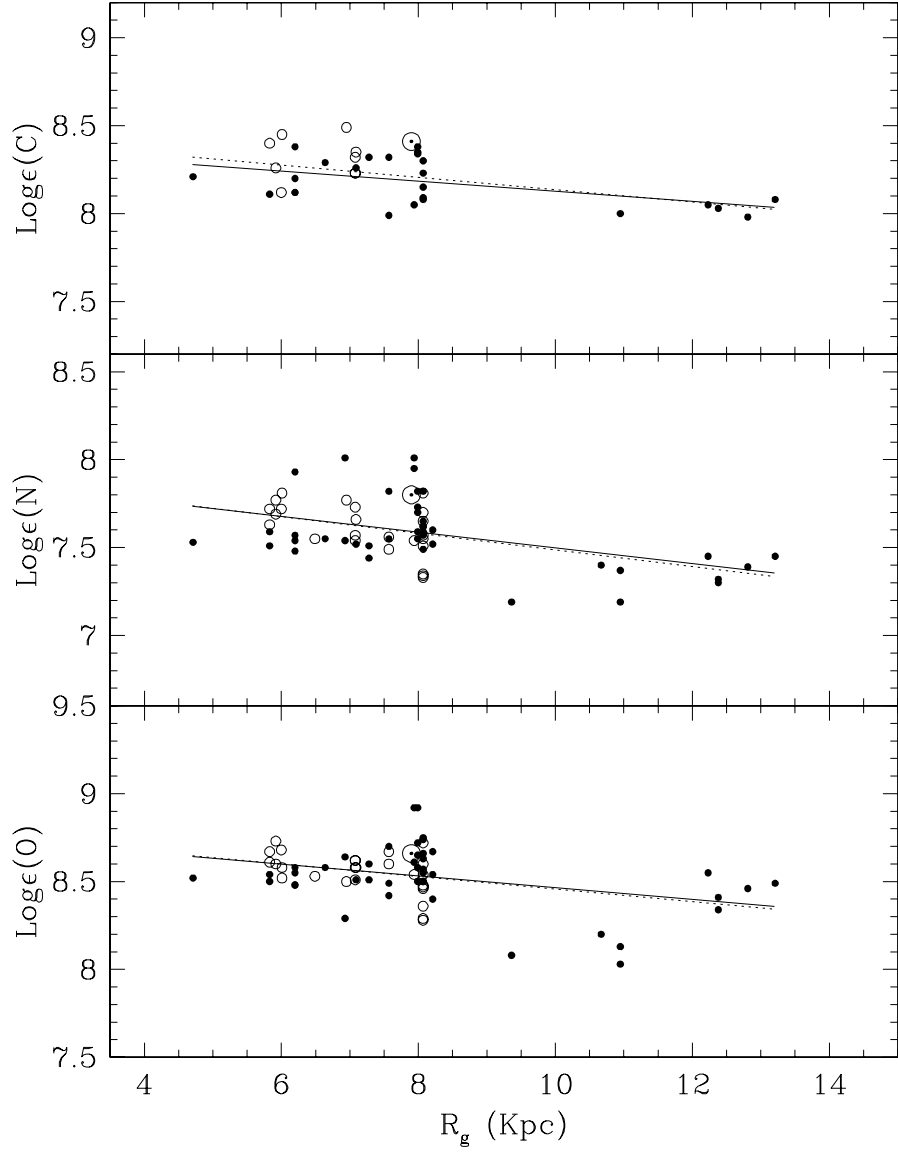


Fig. 4.— A comparison between gradients obtained for the full sample (dotted lines) and a subsample of 43 low $v \sin i$ stars (solid lines). The open circles represent sample stars with high $v \sin i$ and the filled circles low $v \sin i$ stars. The inclusion of high $v \sin i$ stars in our analysis does not introduce any significant biases in the obtained best-fitted slopes.

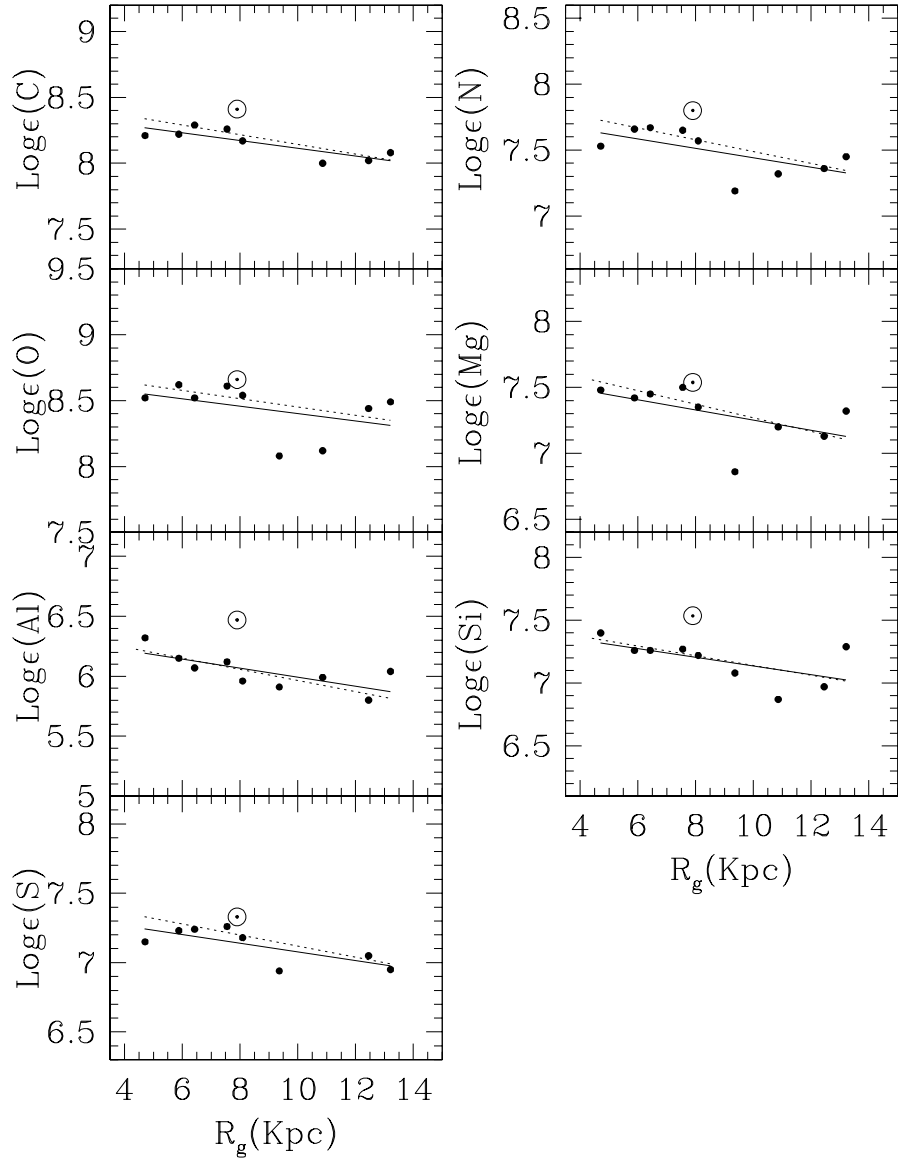


Fig. 5.— Abundance gradients for the sample binned in $\Delta R_g = 1$ kpc (solid lines). The filled circles represent average abundance values for the stars within a bin. The dotted straight lines represent the original gradients presented in Table 3.

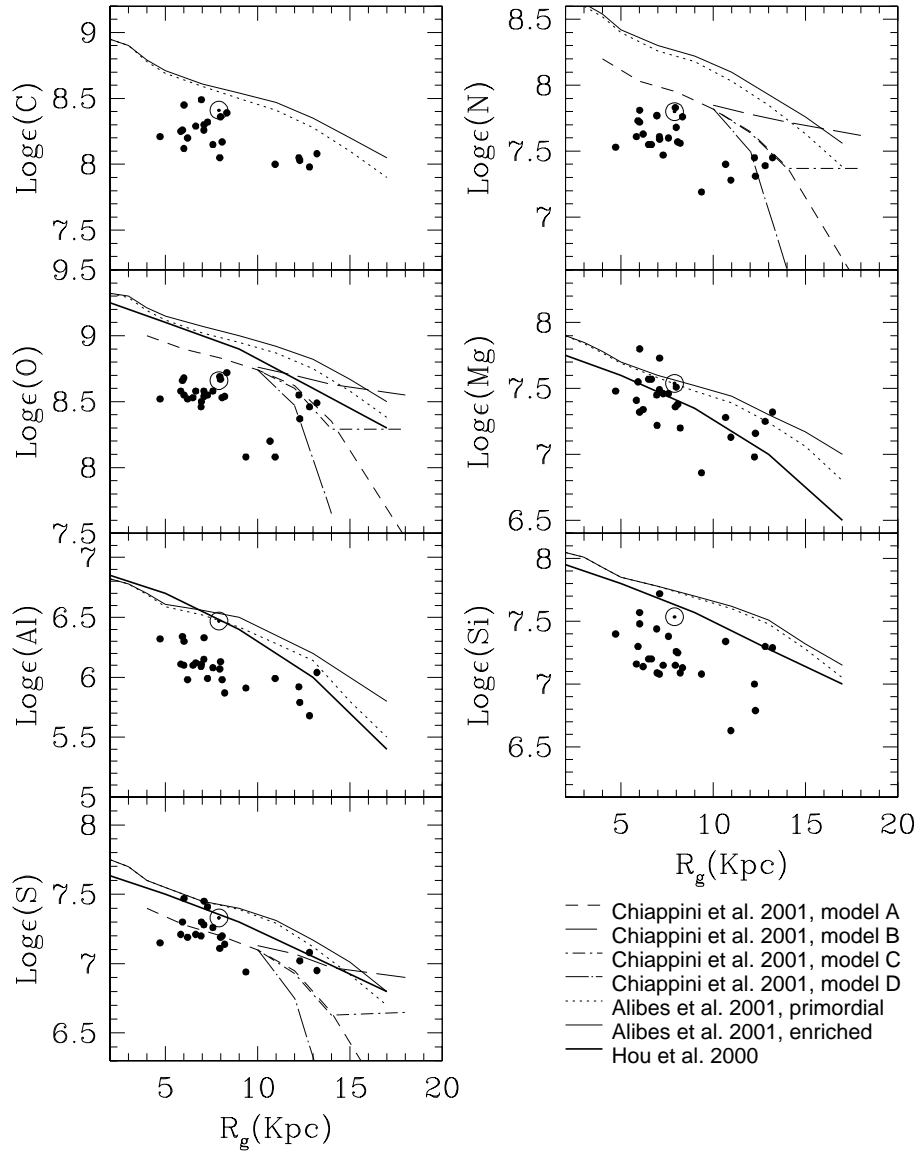


Fig. 6.— Clusters abundances compared to the predicted radial gradients of Hou, Prantzos, & Boissier (2000 - solid thick line), Alibés, Labay, & Canal (2001 - solid and dotted lines) and Chiappini, Matteucci, & Romano (2001 - dashed lines).

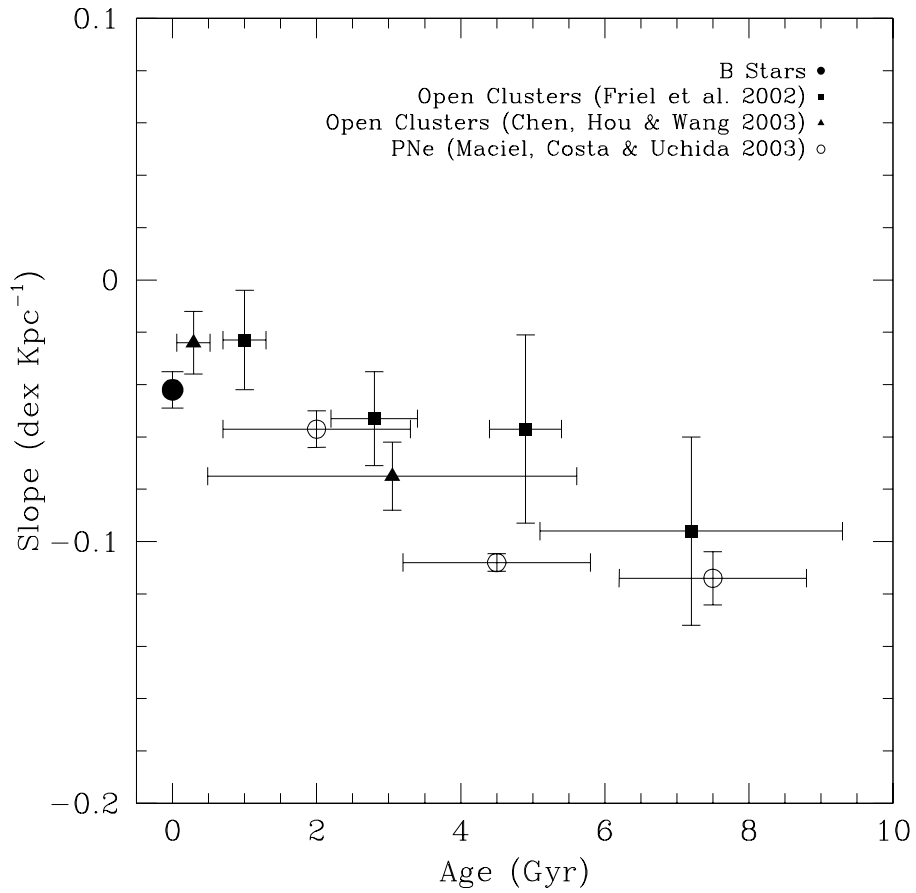


Fig. 7.— The time evolution of the metallicity gradients for the Milky Way disk is shown for [Fe/H] gradients obtained from open clusters and planetary nebulae. The average abundance gradient obtained from our sample of OB stars, which are young, is consistent with the flattening of the metallicity gradients.